# Accommodation of transformation strains in transverse multiferroic nanostructures $CoFe_2O_4$–$PbTiO_3$

Igor Levin[a] and Julia Slutsker
*Materials Science and Engineering Laboratory, National Institute of Standards and Technology, Gaithersburg, Maryland 20899*

Jianhua Li, Zhuopeng Tan, and Alexander L. Roytburd
*Department of Materials Engineering, University of Maryland, College Park, Maryland 20742*

(Received 24 April 2007; accepted 16 July 2007; published online 9 August 2007)

Variable-temperature x-ray diffraction was used to investigate the internal strains that arise from a ferroelectric phase transition in self-assembled multiferroic nanostructures $CoFe_2O_4$–$PbTiO_3$ on (001) $SrTiO_3$. The constraints from $CoFe_2O_4$ suppressed the $c/a$ ratio in tetragonal $PbTiO_3$ (without affecting its Curie temperature) while the expansion of the out-of-plane lattice parameter in $PbTiO_3$ upon the transition induced tensile out-of-plane strain in $CoFe_2O_4$. The transformation strain was partly relieved by the 90° twin domains in $PbTiO_3$ which reduced the net deformation of the component phases. Significant fractions of both *c*- and *a*-domains were observed despite the nanoscale of $PbTiO_3$ in the composite films. © *2007 American Institute of Physics*.
[DOI: 10.1063/1.2768890]

Multiferroic composite films that consist of magnetostrictive and piezoelectric phases arranged in transverse architectures (interphase boundaries perpendicular to the film-substrate interface) exhibit significant magnetoelectric effects due to a reduced clamping by the substrate.[1,2] Such transverse heterostructures can be generated via an epitaxial self-assembly of immiscible but lattice-matched magnetic and ferroelectric phases on single-crystal substrates, as demonstrated recently for several spinel-perovskite systems.[1–3] The resulting nanostructures exhibit a three dimensional epitaxy with phase morphologies determined by the phase fractions and substrate orientation.[4–6]

The strain-mediated magnetoelectric (ME) response of transverse multiferroic nanostructures depends strongly on the efficiency of elastic interactions across the interphase boundaries as well as on the sign and level of residual stresses in the component phases.[7] Residual stresses in the composite spinel-perovskite films originate primarily from the paraelectric → ferroelectric phase transition that occurs in the perovskite phase on cooling from the growth temperature and is accompanied by a significant lattice distortion. Unlike single-phase thin layers on a substrate, the individual phases in the transverse nanostructures are constrained both parallel and perpendicular to the substrate. In the present letter, we used variable-temperature x-ray diffraction to analyze the strain evolution and the effect of constraints on the ferroelectric phase transition in epitaxial self-assembled $CoFe_2O_4$–$PbTiO_3$ films on $SrTiO_3$. We established that, similar to the single-phase ferroelectric layers, the transformation stresses in the composite multiferroic films are partly relaxed through formation of nanoscale twin domains in a ferroelectric phase.

The $x CoFe_2O_4$–$(1-x)PbTiO_3$ films ($x=1/3, 2/3$) were grown from the composite targets having fixed compositions on (001) $SrTiO_3$ substrates ($T=630$ °C) using pulsed lased deposition. The film thicknesses were 230 nm. The $CoFe_2O_4$ (CFO) and $PbTiO_3$ (PTO) phases self-assembled during growth into arrays of $CoFe_2O_4$ pillars dispersed in a $PbTiO_3$ matrix, as detailed in Refs. 3 and 4. A cube-on-cube epitaxy among the $CoFe_2O_4$, $PbTiO_3$, and $SrTO_3$ was confirmed. The films were characterized in an x-ray diffractometer (XRD) equipped with a high-temperature stage. Room-temperature values of the out-of-plane ($a_\perp$) and in-plane ($a_\parallel$) lattice parameters were determined for each phase using four nonequivalent reflections (Cu $K\alpha_1$ radiation). Variable-temperature lattice parameter measurements were conducted using $004_{PTO}/008_{CFO}$ and $220_{PTO}/440_{PTO}$ reflections and Cu $K\alpha$ radiation; the same optical configuration (with a 0.2 mm detector slit) was used for a reciprocal space mapping. XRD patterns for the $CoFe_2O_4$–$PbTiO_3$ films were collected at 25 °C intervals between the ambient temperature and 630 °C. The temperatures were confirmed to be accurate within 5 °C. Heating-cooling cycling in the 25–630 °C range demonstrated that the changes in the lattice parameters were fully reversible. Scanning electron microscopy images of the films recorded before and after their thermal exposure confirmed lack of detectable changes in the nanostructure morphologies during high-temperature x-ray measurements.

Room temperature values of the lattice parameters for $PbTiO_3$ and $CoFeO_4$ are summarized in Table I. At room temperature, the distribution of *d*-spacing values in $PbTiO_3$ was significantly broader than that in $CoFe_2O_4$, as inferred from the relative widths of the $002_{PTO}$ [full width at half

TABLE I. Room temperature values of lattice parameters of $PbTiO_3$ and $CoFe_2O_4$ in the composite $x CoFe_2O_4$–$(1-x)PbTiO_3$ films. The numbers in parentheses represent combined statistical uncertainties ($1\sigma$) from the x-ray profile fitting and least squares refinements using four nonequivalent reflections.

| | $PbTiO_3$ | | $CoFe_2O_4$ | |
|---|---|---|---|---|
| $x$ | $a_\perp$ | $a_\parallel$ | $a_\perp$ | $a_\parallel$ |
| 1/3 | 4.035(1) | 3.945(1) | 8.420(1) | 8.383(1) |
| 2/3 | 4.008(1) | 3.959(1) | 8.396(1) | 8.368(1) |

[a]Electronic mail: igor.levin@nist.gov

 

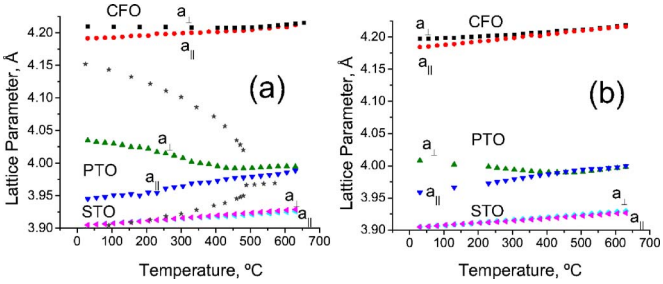


FIG. 1. (Color online) Out-of-plane ($a_\perp$) and in-plane ($a_\parallel$) lattice parameters of $CoFe_2O_4$ (divided by 2), $PbTiO_3$, and $SrTiO_3$ in the $xCoFe_2O_4-(1-x)PbTiO_3$ films on (001) $SrTiO_3$ measured as a function of temperature. (a) $x=1/3$ and (b) $x=2/3$. Lattice parameters of bulk $PbTiO_3$ Ref. 8 are superimposed in Fig. 1 (left) using asterisks.

maximum (FWHM)=0.79°, $x=2/3$] and $004_{CFO}$ (FWHM =0.293°, $x=2/3$), peaks, respectively. The $002_{PTO}$ rocking curve (FWHM=0.79°, $x=2/3$) was also broader than the $004_{CFO}$ rocking curve (FWHM=0.73°, $x=2/3$).

Figure 1 presents results of the variable-temperature lattice parameters measurements in the films with $x=1/3$ [Fig. 1(a)] and $x=2/3$ [Fig. 1(b)]; the data for bulk $PbTiO_3$ (Ref. 8) are superimposed in Fig. 1 (left). An onset of the cubic↔tetragonal phase transition in $PbTiO_3$ is clearly observed at $T_c \approx 450$ °C as a divergence of the $a_\perp(T)$ and $a_\parallel(T)$ lattice parameters. Similar transition temperatures are observed regardless of phase fractions. Previous studies confirmed that the epitaxial stresses that arise during growth are largely accommodated by misfit dislocations.[4] A small tetragonal distortion of $PbTiO_3$ and $CoFe_2O_4$ above $T_c$ (Fig. 2, left) due to the nonrelaxed epitaxial stresses still cannot be ruled out but is difficult to ascertain due to insufficient precision of the in-plane lattice parameter measurements. Above $T_c \approx 450$ °C, the width of the $002_{PTO}$ reflection in the $\theta$-$2\theta$ scans decreases drastically and becomes comparable to that of the $004_{CFO}$; concurrently, the integrated intensities of the $002_{PTO}$ reflections in the $x=1/3$ and $x=1/3$ films increase by the factors of ≈2.25 and ≈3, respectively. In contrast, the integrated intensity of reflection $004_{CFO}$ remains unchanged, regardless of phase fractions. The width of the $002_{PTO}$ rocking curve decreases by nearly a factor of 2 above the transition while some, though much smaller, narrowing of the $004_{CFO}$ rocking curve is observed as well. These results indicate that a broad distribution of the *d*-spacing values along with the broad mosaics, as encountered at room temperature in $PbTiO_3$, is associated with a phase transition rather than a growth process.

The transition temperature for $PbTiO_3$ in the composite films is lower ($\Delta T_c \approx 45$ °C) than that in the bulk crystals

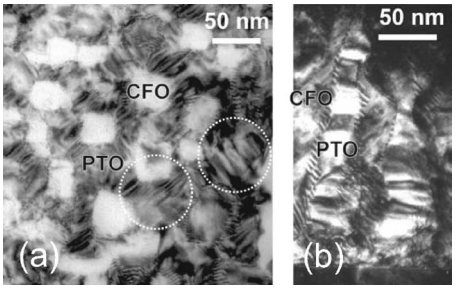


FIG. 2. Plane-view (a) and cross-sectional (b) diffraction-contrast TEM images of the $x=1/3$ film. Twin domains in $PbTiO_3$ are observed.

(495 °C). The tetragonal distortion in $PbTiO_3$ is strongly suppressed yielding the $c/a$ ratio (room temperature) of only ≈1.023 for $x=1/3$ and ≈1.013 for $x=2/3$ as opposed to $c/a \approx 1.064$ for a bulk $PbTiO_3$. The constraints from $CoFe_2O_4$ suppress the jump of the $PbTiO_3$ lattice parameters at the transition point thereby modifying the character of this transition from the strongly first order toward a more continuous like type; the effect becomes stronger with increasing volume fraction of $CoFe_2O_4$. At the same time, an expansion of the *c*-lattice parameter in $PbTiO_3$ induced a tetragonal distortion $a_\perp/a_\parallel > 1$ in $CoFe_2O_4$. The room temperature value of this distortion varies from 1.004 for $x=1/3$ to 1.003 for $x=2/3$. As expected from the stress equilibrium conditions, the out-of-plane strains in $CoFe_2O_4$ decrease with a volume fraction of this phase increasing, while a reciprocal trend is observed for the strains in $PbTiO_3$. The suppressed $c/a$ ratio is expected to reduce the spontaneous out-of-plane polarization in $PbTiO_3$ compared to its strain-free bulk value.

The effect of elastic constraints on the Curie temperature of a ferroelectric in the composite film can be predicted by considering a free energy expansion for a constrained ferroelectric film on a substrate $F=A(T-T_0)P^2+BP^4+CP^6+F_{el}$, where *A*, *B*, and *C* are the Landau coefficients and $F_{el}$ is the elastic energy of the film. The $F_{el}$ of a film consisting of cylindrical magnetic rods embedded into a ferroelectric matrix was calculated previously.[5,7] Neglecting the self-strain of a magnetic phase, this energy can be expressed as $F_{el}=[\alpha G Q_{11}^2(1-\delta)(1+\delta-2\nu\delta)+GQ_{11}^2 2\delta^2(1+\nu)]P^4$, where $\alpha$ is a fraction of a magnetic phase, *G* is the in-plane elastic modulus of the film, $\nu$ is a Poisson ratio, $Q_{11}$ and $Q_{12}$ are electrostrictive coefficients of a ferroelectric phase, and $\delta=Q_{12}/Q_{11}$. Evidently, the energy associated with the interphase elastic interactions modifies just the $P^4$ term in the free energy expansion and thus has no effect on the Curie temperature of a ferroelectric. Yet, this elastic energy affects the sign of the $P^4$ term thereby changing the character of a ferroelectric phase transition from the first to second order, consistent with the experimental observations (Fig. 1). The change in the $T_c$ associated with this change in the order of the transition is expected to be ≈13 °C.[9]

Reduced values of a ferroelectric transition temperature in the composite films can be readily attributed to a limited but detectable dissolution of Fe in $PbTiO_3$, reported previously.[4] Dissolution of Ti in $CoFe_2O_4$ also was observed,[4] consistent with a complete solubility among $CoFe_2O_4$ and $Co_2TiO_4$.[10] Concurrently, the transformation strain (and the resulting strain-free $c/a$ ratio) for the $Pb(Ti,Fe)O_{3-\delta}$ solid solutions in the $CoFe_2O_4-PbTiO_3$ nanostructures should be reduced compared to the pure $PbTiO_3$.[11] The uncertainties in the reference (strain-free) states of the component phases caused by formation of the solid solutions preclude accurate determination of residual strains in the composite nanostructures; yet variable-temperature measurements provide an insight into the strain accommodation mechanism as discussed below.

Strain compatibility conditions along the $CoFe_2O_4/PbTiO_3$ interfaces imply equal changes of the out-of-plane lattice parameters of $CoFe_2O_4$ and $PbTiO_3$ from their respective values in the cubic state just prior to a ferroelectric phase transition. However, the expansion of $a_\perp$ in $PbTiO_3$, as observed in Fig. 2, exceeds significantly the out-of-plane strain in $CoFe_2O_4$. Considering a reversibility of the lattice parameters upon the heating/cooling cycles, this dis-

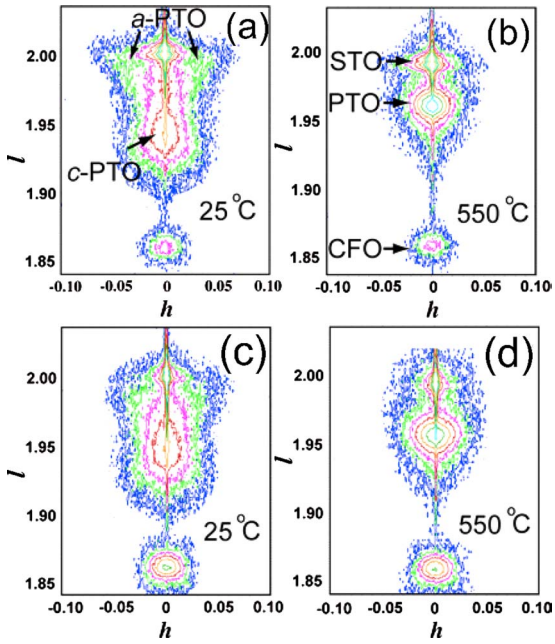


FIG. 3. (Color online) Low-resolution reciprocal space maps encompassing 200 $SrTiO_3$, 002/200 $PbTiO_3$, and 400 $CoFe_2O_4$ reflections for films with [(a) and (b)] $x=1/3$ and [(c) and (d)] $x=2/3$ acquired at [(a) and (c)] 25 °C [(b) and (d)] and 550 °C. Appearance of the *a* domains in $PbTiO_3$ below a ferroelectric transition can be observed.

crepancy can be accounted for by formation of the 90° twin domains in $PbTiO_3$. Indeed, such 90° domains were identified using both diffraction-contrast imaging in a transmission electron microscope (TEM) (Fig. 2) and XRD (Fig. 3). The $PbTiO_3$ was confirmed to contain four *a*-domain variants in addition to the *c*-domains. Naturally, the average out-of-plane deformation in $PbTiO_3$ is significantly smaller than that observed just for the *c*-domains in Fig. 1.

A volume fraction of the *c*-domains $\beta$ estimated from the relative integrated intensities of the 001 and 100(×4) peaks in the x-ray diffraction rocking curves was approximately 0.5; however, the accuracy of these measurements is limited by the relatively poor separation of the broad *a*-domain peaks. Alternatively, a volume fraction of the *c*-domains can be calculated from the experimental data in Fig. 1 by considering the strain compatibility conditions for a composite film: (1) $\varepsilon_{33}^{\mathrm{CFO}}=\varepsilon_{33}^{\mathrm{PTO}}$ and (2) $\alpha\varepsilon_{11}^{\mathrm{CFO}}+(1-\alpha)\varepsilon_{11}^{\mathrm{PTO}}=\varepsilon_s$, where $\varepsilon_{33}^{\mathrm{CFO}}/\varepsilon_{11}^{\mathrm{CFO}}$ and $\varepsilon_{33}^{\mathrm{PTO}}/\varepsilon_{11}^{\mathrm{PTO}}$ are the out-of-plane/in-plane total strains in the $CoFe_2O_4$ and $PbTiO_3$ phases, respectively, $\varepsilon_s$ describes a thermal contraction of the substrate, and $\alpha$ is a volume fraction of $CoFe_2O_4$. Assuming an equilibrium domain structure, where all domains have identical $c/a$ ratios,[12] and using the out-of-plane strain compatibility condition (1), a fraction of the *c*-domains $\beta$ can be calculated as $\beta=(\varepsilon_{33}^{\mathrm{CFO}}-\varepsilon_a)/(\varepsilon_c-\varepsilon_a)$, where $\varepsilon_c=(a_\perp-a_0)/a_0$ and $\varepsilon_a=(a_\parallel-a_0)/a_0$ (here $a_\perp$ and $a_\parallel$ are the experimental room-temperature values of the $PbTiO_3$ lattice parameters and $a_0$ is the lattice parameter of the cubic $PbTiO_3$ just above the transition). The *c*-domain fractions calculated using experimental values of the lattice parameters (Fig. 1) are 0.61 and 0.51 for $\alpha=1/3$ and $\alpha=2/3$, respectively, which agrees well with the estimates made from the rocking curve measurements. Substituting these values of $\beta$ into the second, in-plane strain condition yields values of −0.002 ($\alpha=1/3$) and −0.004 ($\alpha=2/3$) which reflect a combination of the substrate contraction ($\varepsilon_s=0.006$) and stress heterogeneities not accounted for by the above expression for $\beta$. Overall, our results support presence of significant fractions of both *c*- and *a*-domains in $PbTiO_3$, despite a nanoscale of the composite heterostructures. Small domain size contributes to a broadening of the $PbTiO_3$ reflections.

A substantial fraction of *a*-domains which dilute the net out-of-plane polarization in $PbTiO_3$ is expected to reduce the strength of electromagnetic $E(H)$ coupling compared to the theoretical estimates made for a single-domain $PbTiO_3$.[7] However, the effect of these domains on the magnitude of a magnetoelectric $M(E)$ coupling will depend on the mobility of domain walls which requires further investigation; in principle, the ME coupling can be enhanced providing the domain walls are sufficiently mobile. Clearly, the optimal choice of a ferroelectric component for a given nanostructure architecture should consider a relief mechanism for the transformation stresses.

[1] H. Zheng, J. Wang, S. E. Lofland, Z. Ma, L. Mohaddes-Ardabili, T. Zhao, L. Salamanca-Riba, S. R. Shinde, S. B. Ogale, F. Bai, D. Viehland, Y. Jia, D. G. Schlom, M. Wuttig, A. Roytburd, and R. Ramesh, Science **303**, 661 (2004).
[2] F. Zavaliche, H. Zheng, L. Mohaddes-Ardabili, S. Y. Yang, Z. Qhan, P. Shafer, E. Reilly, R. Chopdekar, Y. Jia, P. Wright, D. Schlom, G. Y. Suzuki, and R. Ramesh, Nano Lett. **5**, 1793 (2005).
[3] J. Li, I. Levin, J. Slutsker, V. Provenzano, P. K. Schenk, R. Ramesh, J. Ouyang, and A. L. Roytburd, Appl. Phys. Lett. **87**, 072909 (2005).
[4] I. Levin, J. Li, J. Slutsker, and A. L. Roytburd, Adv. Mater. (Weinheim, Ger.) **18**, 2044 (2006).
[5] J. Slutsker, I. Levin, J. Li, A. Artemev, and A. L. Roytburd, Phys. Rev. B **73**, 184127 (2006).
[6] H. Zheng, Q. Zhan, F. Zavaliche, M. Sherburne, F. Straub, M. P. Cruz, L. Q. Chen, U. Dahmen, and R. Ramesh, Prog. Biophys. Biophys. Chem. **6**, 1401 (2006).
[7] J. Slutsker, Z. Tan, A. L. Roytburd, and I. Levin, J. Mater. Res. **22**, 8 (2007).
[8] M. J. Haun, E. Furman, S. J. Jang, H. A. McKinstry, and L. E. Cross, J. Appl. Phys. **62**, 3331 (1987).
[9] M. J. Haun, E. Furman, H. A. McKinstry, and L. E. Cross, Ferroelectrics 99, **27** (1989).
[10] V. R. Palkar and S. K. Malik, Solid State Commun. **134**, 783 (2005).
[11] P. Nathwani and V. S. Darshane, J. Phys. C **21**, 3191 (1988).
[12] A. L. Roytburd and J. Slutsker, J. Mech. Phys. Solids **49**, 1795 (2001).